

Quantum phase transitions of 2-d dimerized spin-1/2 Heisenberg models with spatial anisotropy

M.-T. Kao,¹ D.-J. Tan,¹ and F.-J. Jiang^{1,*}

¹*Department of Physics, National Taiwan Normal University, 88, Sec.4, Ting-Chou Rd., Taipei 116, Taiwan*

Motivated by the unexpected Monte Carlo results as well as the theoretical proposal of a large correction to scaling for the critical theory of the 2-d staggered-dimer spin-1/2 Heisenberg model on the square lattice, we study the phase transitions induced by dimerization of several dimerized quantum Heisenberg models with spatial anisotropy using first principles Monte Carlo method. Remarkably, while our Monte Carlo data for all the models considered here, including the herringbone- and ladder-dimer models on the square lattice, are compatible with the recently proposed scenario of an enhanced correction to scaling, we find it is likely that the enhanced correction to scaling manifests itself as amplification of the nonuniversal prefactors appeared in the scaling forms. In other words, our data are in consistence with the established numerical values for the critical exponents, including the confluent exponent, in the $O(3)$ universality class. Convincing numerical evidence is provided to support this proposed scenario.

I. INTRODUCTION

While being well-studied and understood thoroughly, the dimerized quantum Heisenberg models with spatial anisotropy have triggered theoretical interests again recently [1–12]. For example, the 3-d spatially anisotropic quantum Heisenberg model with a ladder dimerization pattern is used to demonstrate a universal behavior, which is argued to be relevant for understanding the experimental results of the material TlCuCl_3 [13]. Further, the 2-d dimerized spin-1/2 Heisenberg model with a spatially staggered anisotropy is of particularly interesting because this model seems to establish an unconventional phase transition [14]. Specifically, although it is believed that the phase transition induced by dimerization for this model should be governed by the $O(3)$ universality class theoretically [15–19], a recent large scale Monte Carlo calculation obtains $\nu = 0.689(5)$ and $\beta/\nu = 0.545(5)$, which are in contradiction to the established $O(3)$ results $\nu = 0.7112(5)$ and $\beta/\nu = 0.519(1)$ in the literature [20]. Here ν and β are the critical exponents corresponding to the correlation length and the magnetization, respectively. In order to clarify this issue further, several efforts have been devoted to study the phase transition of this model induced by dimerization. For instance, an unconventional finite-size scaling is proposed in [21]. Further, in [22] it is argued that, due to a cubic term, there is a large correction to scaling for this phase transition which results in the unexpected $\nu = 0.689(5)$ and $\beta/\nu = 0.545(5)$ obtained in [14]. Later, a Monte Carlo study indeed provides strong evidence to support this scenario of an enhanced correction to scaling [21]. In addition to the staggered-dimer spin-1/2 Heisenberg model on the square lattice, in [22] it concludes as well that a similar model on the honeycomb lattice, which is de-

picted in the bottom panel of figure 1¹, as well as the herringbone-dimer model on the square lattice (middle panel of figure 1) also belong to the same category of models receiving an enhanced correction. This general picture regarding the correction to scaling for 2-d dimerized quantum Heisenberg models is indeed supported by several related Monte Carlo studies [3, 23–26].

While all the available Monte Carlo results provide convincing evidence for the proposal of an enhanced correction to scaling, the good scaling property of the observable $\rho_{s_2}2L$ for the staggered-dimer model on the square lattice is the most noticeable observation [21], where again ρ_{s_2} and L are the spin stiffness in the 2-direction and the spatial box size employed in the simulations, respectively. Inspired by this observation, one naturally would like to examine whether for the staggered-dimer model on the honeycomb lattice and the herringbone-dimer model on the square lattice, a similar good scaling behavior will be observed when considering the same observable $\rho_{s_2}2L$ for these two dimerized models. Although the phase transition induced by dimerization of the staggered-dimer model on the honeycomb lattice has been studied before, a detailed comparison between the scaling behavior of $\rho_{s_1}2L$ and $\rho_{s_2}2L$ as well as the relevant investigation of the exponent β/ν are not available yet [27]. In addition, to examine how the enhanced correction to scaling, due to a cubic irrelevant term as suggested in [22], affects the determination of the exponents ν and β/ν for the staggered- and herringbone-dimer models is an interesting topic to explore as well [28]. Indeed, whether the cubic term will influence the numerical value of the confluent exponent ω has not explored in [22]. Hence in this study, we have investigated the phase transitions of the herringbone- and ladder-dimer spin-1/2 Heisenberg models on the square

*fjiang@ntnu.edu.tw

¹ We will call this model the staggered-dimer model as well unless confusion arises.

lattice, as well as the quantum staggered-dimer model on the honeycomb lattice. In particular, the largest lattice sizes reached here are as twice large as those of the relevant early studies in some cases. The results for the ladder-dimer model are included here for completeness and comparison purpose, since the enhanced correction to scaling should be absent for this model. Remarkably, as we will demonstrate later, indeed $\rho_{s2}2L$ of the staggered-dimer model on the honeycomb lattice shows a good scaling behavior. Consequently, we are able to obtain a value for ν , in agreement with the established $\nu = 0.7112(5)$ in the $O(3)$ universality class, by employing the leading scaling ansatz in our finite-size scaling analysis for $\rho_{s2}2L$. Interestingly, while our Monte Carlo data for all the models studied here, including the herringbone- and ladder-dimer models on the square lattice, are compatible with the recently proposed scenario of an enhanced correction to scaling for the phase transitions considered here, we find that the enhanced correction to scaling manifests itself as amplification of the nonuniversal prefactors appeared in the scaling forms. In other words, our data are in consistency with the established results of $\nu = 0.7112(5)$, $\beta/\nu = 0.519(1)$, and $\omega \sim 0.78$ in the $O(3)$ universality class. We provide numerical evidence to support this proposed scenario of amplification of the nonuniversal prefactors appeared in the scaling forms, by demonstrating that the values of ω for the herringbone- and staggered-dimer models are compatible with $\omega \sim 0.78$, through a calculation of relevant observables at the corresponding critical points.

This paper is organized as follows. First, after an introduction, the spatially anisotropic quantum Heisenberg models and the relevant observables studied in this work are briefly described, after which we present our numerical results. In particular, the results obtained from the finite-size scaling analysis are discussed in detail. A final section then concludes our study.

II. MICROSCOPIC MODEL AND CORRESPONDING OBSERVABLES

The Heisenberg models considered in this study are defined by the Hamilton operator

$$H = \sum_{\langle xy \rangle} J \vec{S}_x \cdot \vec{S}_y + \sum_{\langle x'y' \rangle} J' \vec{S}_{x'} \cdot \vec{S}_{y'}, \quad (1)$$

where J and J' are antiferromagnetic exchange couplings connecting nearest neighbor spins $\langle xy \rangle$ and $\langle x'y' \rangle$, respectively. Figure 1 illustrates the models which are described by Eq. (1) and are investigated in great detail here. To study the critical behavior of these models near the transition driven by the anisotropy, in particular, to determine the critical points as well as the critical exponent ν , the spin stiffnesses in the 1- and 2-directions which are defined by

$$\rho_{si} = \frac{1}{\beta L^2} \langle W_i^2 \rangle, \quad (2)$$

are measured in our simulations. Here β is the inverse temperature and L again refers to the spatial box size. Further $\langle W_i^2 \rangle$ with $i \in \{1, 2\}$ is the winding number squared in the i direction. In addition, the second Binder ratio Q_2 , which is defined by

$$Q_2 = \frac{\langle (m_s^z)^2 \rangle^2}{\langle (m_s^z)^4 \rangle}, \quad (3)$$

is also measured in our simulations as well. Here m_s^z is the z component of the staggered magnetization $\vec{m}_s = \frac{1}{L^2} \sum_x (-1)^{x_1+x_2} \vec{S}_x$. By carefully investigating the spatial volume and the J'/J dependence of $\rho_{si}L$ as well as Q_2 , one can determine the critical points and the critical exponent ν with high precision. Finally the exponent β/ν is determined by studying the scaling behavior of the observables $\langle |m_s^z| \rangle$ and $\langle (m_s^z)^2 \rangle$, which are measured in this study as well, at the corresponding critical points.

III. DETERMINATION OF THE CRITICAL POINTS AND THE CRITICAL EXPONENT ν

To study the quantum phase transitions of our central interest, we have carried out large scale Monte Carlo simulations using a loop algorithm [29–33]. Further, to calculate the relevant critical exponent ν and to determine the location of the critical points in the parameter space J'/J for the models described by figure 1, we have employed the technique of finite-size scaling for certain observables. For example, if a transition is second order, then at low-temperature² and near the transition the observable $\rho_{si}2L$ for $i \in \{1, 2\}$ and Q_2 should be described well by the following finite-size scaling ansatz [34–38]

$$\begin{aligned} \mathcal{O}_L(t) &= g_{\mathcal{O}}(tL^{1/\nu}, \Delta^{-1}/\beta, r) + L^{-\omega} g_{\mathcal{O}\omega}(tL^{1/\nu}, \Delta^{-1}/\beta, r) \\ &= g_{\mathcal{O}}(tL^{1/\nu}, \Delta^{-1}/\beta, r) \times \\ &\quad \left(1 + L^{-\omega} g'_{\mathcal{O}\omega}(tL^{1/\nu}, \Delta^{-1}/\beta, r) \right) \end{aligned} \quad (4)$$

where \mathcal{O}_L stands for Q_2 and $\rho_{si}L$ with $i \in \{1, 2\}$, L is the lattice size in the 1-direction, $t = (j_c - j)/j_c$ with $j = (J'/J)$, ν is the critical exponent corresponding to the correlation length ξ , ω is the confluent correction exponent, Δ is the energy gap which scales as $\Delta \sim 1/L^z$ with z being the dynamical critical exponent (which is 1 for the phase transitions considered here), and r is the ratio of the lattice size in the 1- and 2-direction. Further, $g_{\mathcal{O}}$, $g_{\mathcal{O}\omega}$, and $g'_{\mathcal{O}\omega}$ appearing above are smooth functions of the variables $tL^{1/\nu}$, Δ^{-1}/β , and r . In practice one would carry out the analysis close to the critical point so that $g'_{\mathcal{O}\omega}$ in Eq. (4) can be approximated by a constant.

² Specifically, one expects that the temperature should be lower than the energy gap $\Delta \sim 1/L$ for the systems considered in this study.

Specifically, the following ansatz

$$\mathcal{O}_L(t) = (1 + bL^{-\omega})g_{\mathcal{O}}(tL^{1/\nu}, L^z/\beta, r), \quad (5)$$

where b is some constant, is frequently used when applying the finite-size scaling technique. While Eq. (5) is only valid for large box sizes and close to the critical point, to present the main results of this study we find it is sufficient to employ Eq. (5) for the data analysis. Notice that for square lattice or rectangular-shape lattice with a fixed r , one will intuitively neglect the effect of r in Eq. (5). Hence, we will apply Eq. (5) with a constant r to the relevant observables for obtaining $(J'/J)_c$ and ν . Notice from Eq. (5), one concludes that the curves for \mathcal{O}_L corresponding to different L , as functions of J'/J , should intersect at the critical point $(J'/J)_c$ for large L . Without loss of generality, we have fixed $J = 1$ in our simulations and have varied J' . Additionally, the box size used in the simulations ranges from $L = 24$ to $L = 136$ (Strictly speaking, $L = \sqrt{N}$ for the staggered-dimer model on the honeycomb lattice. Here N is the number of spins used in the simulations). Notice to eliminate the temperature dependence in Eq. (5), one naturally would use large enough inverse temperature β in the simulations so that all the considered observables take their zero-temperature values. On the other hand, since Eq. (5) is valid for sufficiently low temperature, one can optimize the ratio of β and L in order to reach a lattice size as large as possible. As a result, we use $\beta J = 2L$ for each L in our simulations so that the temperature dependence in Eq. (5) drops out. We have generated some data using lower temperature and these new data points lead to consistent results with those determined by employing the data obtained with $\beta J = 2L$. First of all, let us focus on our results for the staggered-dimer spin-1/2 Heisenberg model on the honeycomb lattice.

A. Results for the staggered-dimer spin-1/2 Heisenberg model on the honeycomb lattice

Figure 2 shows the Monte Carlo data of $\rho_{s1}2L$, $\rho_{s2}2L$, and Q_2 with $24 \leq L \leq 96$ as functions of J'/J for the staggered-dimer spin-1/2 Heisenberg model on the honeycomb lattice. The figure clearly indicates that the phase transition is most likely second order since for all the observables $\rho_{s1}2L$, $\rho_{s2}2L$, and Q_2 , the curves of different L tend to intersect near a particular point in the parameter space J'/J . A surprising observation from figure 2 is that, while $\rho_{s1}2L$ receives a sizable correction to its scaling (which has already been shown in [26]), the observable $\rho_{s2}2L$ shows a good scaling behavior. Specifically, the correction to scaling for $\rho_{s2}2L$ is negligible for $L \geq 32$. These findings are similar to the scenario regarding the correction to scaling for the same observables, namely $\rho_{s1}2L$ and $\rho_{s2}2L$, of the staggered-dimer model on the square lattice [21]. Indeed, from $\rho_{s2}2L$ with $L \geq 32$, we are able to reach a value for ν compatible with the expected $\nu = 0.7112(5)$ using the lead-

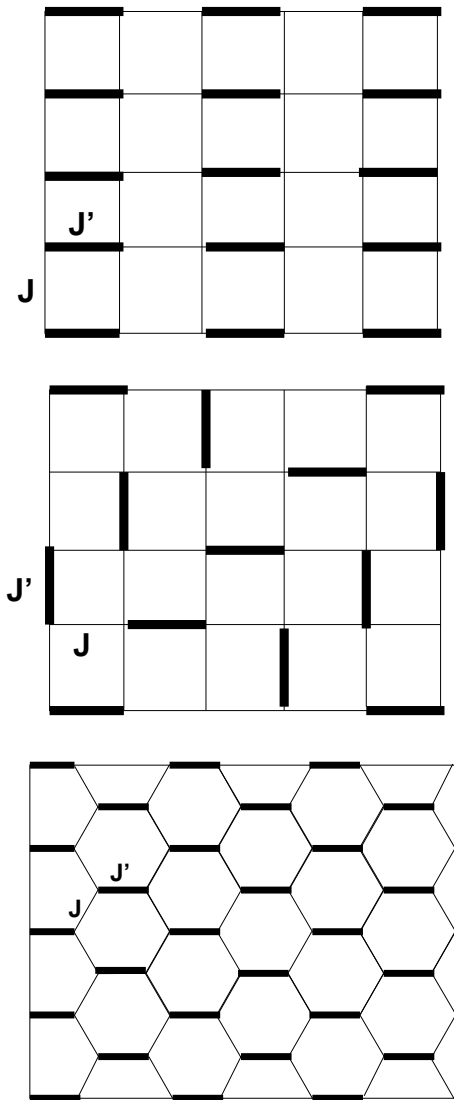


FIG. 1: The dimerized quantum Heisenberg models with spatial anisotropy considered in this study.

ing finite-size scaling ansatz in Eq. (5) (letting $b = 0$ in Eq. (5)). For example, the ν obtained from applying a second order Taylor expansion in $tL^{1/\nu}$ of Eq. (5) with $b = 0$ to the observable $\rho_{s2}2L$ with $40 \leq L \leq 96$ is given by $\nu = 0.7167(40)$, which is in nice agreement with its theoretical expectation in the literature. To reach a value for ν consistent with $\nu = 0.7112(5)$ using the leading finite-size scaling ansatz and the observable $\rho_{s1}2L$, one has to use data with fairly large L as indicated in [26]. Indeed a similar conclusion is reached here. Interestingly, with the observable $\rho_{s1}2L$, while we either arrive at values of ν statistically different from $\nu = 0.7112(5)$ or cannot reach good results when b and ω in Eq. (5) are included as fitting parameters, compatible results of ν with $\nu = 0.7112(5)$ can be obtained from the fits with the assumption that $\omega \leq 0.5$ is used as a criterion for the

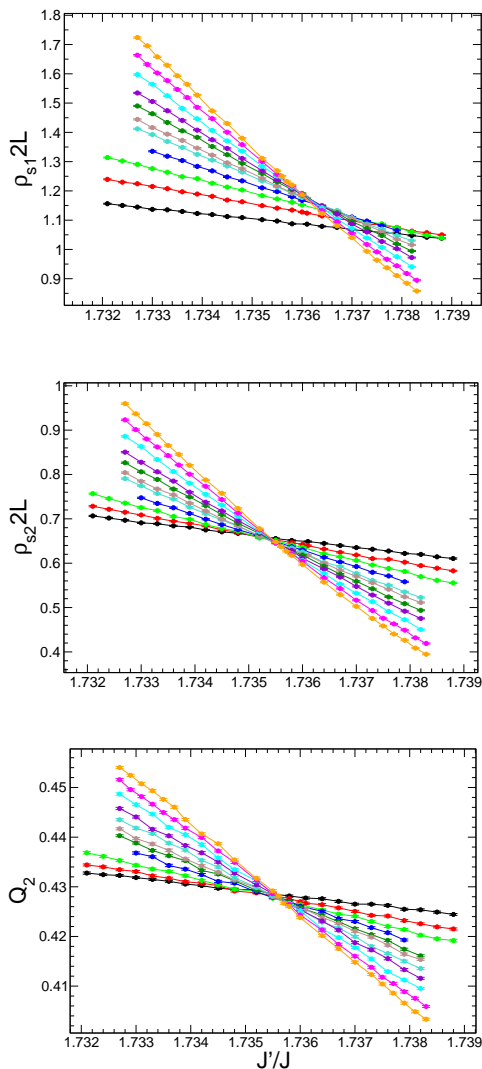


FIG. 2: Monte Carlo data of $\rho_{s1}2L$, $\rho_{s2}2L$, and Q_2 with $24 \leq L \leq 96$ for the staggered-dimer spin-1/2 Heisenberg model on the honeycomb lattice.

fits. For instance, using $\rho_{s1}2L$ with $40 \leq L \leq 96$, the values of ν and ω determined from the fits by employing the criterion of $\omega \leq 0.5$ are given by $\nu = 0.7054(45)$ and $\omega = 0.42(8)$, respectively. Notice $\omega \sim 0.42$ is smaller than the expected $\omega \sim 0.78$ in the $O(3)$ universality class. One might conclude that, our results are consistent with the scenario outlined in [22] that the correction to scaling for this model is enhanced due to a cubic irrelevant term, and this term has impact on the numerical value of ω . Finally, from Q_2 with $32 \leq L \leq 96$, a fit using Taylor expansion to second order in $tL^{1/\nu}$ as well as letting $b = 0$ in Eq. (5) leads to $\nu = 0.7102(56)$ and $(J'/J)_c = 1.73560(4)$, both of which agree quantitatively with the known results in the literature. Interestingly, the obtained coefficients for $(tL^{1/\nu})^2$ in the fits associated with Q_2 are very small. Hence, we can even reach a value for ν in agreement with $\nu = 0.7112(5)$ using a first

observable	L	ν	$(J'/J)_c$	χ^2/DOF
$\rho_{s1}2L$	$40 \leq L \leq 96$	0.7054(45)	1.7355(2)	1.2
$\rho_{s1}2L$	$48 \leq L \leq 96$	0.7096(55)	1.7355(3)	1.2
$\rho_{s2}2L$	$32 \leq L \leq 96$	0.7156(40)	1.73545(3)	1.9
$\rho_{s2}2L$	$40 \leq L \leq 96$	0.7167(40)	1.73548(3)	1.4
$\rho_{s2}2L$	$48 \leq L \leq 96$	0.7055(42)*	1.73550(3)*	0.9
$\rho_{s2}2L$	$56 \leq L \leq 96$	0.7082(45)*	1.73551(3)*	0.9
Q_2	$32 \leq L \leq 96$	0.7102(56)	1.73560(4)	1.4
Q_2	$40 \leq L \leq 96$	0.712(6)	1.73570(5)	1.3
Q_2	$32 \leq L \leq 96$	0.7107(56) $^\diamond$	1.73564(3) $^\diamond$	1.4
Q_2	$40 \leq L \leq 96$	0.712(6) $^\diamond$	1.73566(4) $^\diamond$	1.4

TABLE I: The numerical values of ν and $(J'/J)_c$ calculated from $\rho_{s1}2L$, $\rho_{s2}2L$, and Q_2 for the staggered-dimer model on the honeycomb lattice. All results are obtained by using a second order Taylor expansion in $tL^{1/\nu}$ of Eq. (5) except those with a star (diamond) which are determined by a third order (first order) Taylor expansion. The confluent correction is included in the fit explicitly only for $\rho_{s1}2L$ and is assumed to satisfy the condition $\omega \leq 0.5$.

order Taylor expansion in $tL^{1/\nu}$ of Eq. (5) to fit the data points of Q_2 (the last 2 rows in table 1). The values of ν and $(J'/J)_c$ obtained from the fits mentioned above are listed in table 1. Notice that the uncertainties of $(J'/J)_c$ and ν shown in table 1, as well as in tables 2, 3, 4, and 5 in the following sections, are determined by a conservative estimate based on the standard deviations obtained from the bootstrap resampling method employed for the fits.

B. Results for the herringbone-dimer spin-1/2 Heisenberg model on the square lattice

After having calculated $(J'/J)_c$ and ν for the phase transition induced by dimerization of the staggered-dimer spin-1/2 Heisenberg model on the honeycomb lattice, we turn to investigating the corresponding critical theory of the herringbone-dimer model on the square lattice. Since for this model one has $\rho_{s1} = \rho_{s2}$, the relevant observables used in our finite-size scaling analysis are $\rho_s L$, which is the average of $\rho_{s1}L$ and $\rho_{s2}L$, and the second Binder ratio Q_2 (figure 3). To calculate ν , we first carry out several analysis by employing the second order Taylor expansion in $tL^{1/\nu}$ of Eq. (5), with the sub-leading correction included explicitly, to fit our Monte Carlo data of $\rho_s L$ with variant range of L . Remarkably, a numerical value of ν compatible with $\nu = 0.7112(5)$ can be obtained if the smallest and largest box sizes used in the fits are larger than 24 and 96, respectively. The results of $(J'/J)_c$ and ν calculated from these fits are listed as the first 5 rows in table 2. Further, the values of ω determined from these fits ranges from 0.58 to 0.79 with an average of 0.66. Notice $\omega \sim 0.66$ we ob-

observable	L	ν	$(J'/J)_c$	χ^2/DOF
$\rho_s L$	$24 \leq L \leq 136$	0.705(2)	2.49804(8)	1.4
$\rho_s L$	$24 \leq L \leq 96$	0.706(3)	2.4980(2)	1.4
$\rho_s L$	$24 \leq L \leq 72$	0.702(5)	2.4980(5)	1.1
$\rho_s L$	$32 \leq L \leq 136$	0.706(2)	2.49805(10)	1.4
$\rho_s L$	$32 \leq L \leq 96$	0.707(3)	2.4980(3)	1.4
$\rho_s L$	$24 \leq L \leq 72$	0.700(4)*	2.49813(10)*	1.1
$\rho_s L$	$32 \leq L \leq 136$	0.706(2)*	2.49806(3)*	1.5
$\rho_s L$	$32 \leq L \leq 96$	0.707(3)*	2.49806(7)*	1.4
Q_2	$24 \leq L \leq 136$	0.714(4)	2.49800(7)	0.9
Q_2	$32 \leq L \leq 136$	0.715(6)	2.4980(2)	1.1
Q_2	$24 \leq L \leq 136$	0.710(4)*	2.49820(6)*	1.1
Q_2	$24 \leq L \leq 96$	0.716(5)*	2.4983(1)*	1.1
$\rho_s L$	$24 \leq L \leq 136$	0.701(2)	2.49803(7)	1.2
$\rho_s L$	$32 \leq L \leq 136$	0.702(3)	2.4980(1)	1.2
Q_2	$24 \leq L \leq 136$	0.707(4)	2.49800(15)	0.8
Q_2	$32 \leq L \leq 136$	0.7075(45)	2.4980(2)	0.9
Q_2	$32 \leq L \leq 136$	0.7056(40)*	2.49810(6)*	0.9
Q_2	$40 \leq L \leq 136$	0.7065(40)*	2.49810(7)*	0.8

TABLE II: The numerical values of ν and $(J'/J)_c$ calculated from $\rho_s L$ and Q_2 for the herringbone-dimer model on the square lattice. While the results presented in the first twelve rows are obtained by using a second order Taylor expansion in $tL^{1/\nu}$ of Eq. (5), those listed in the last six rows are determined with a third order Taylor expansion. Further, all results are calculated with the ω and b in Eq. (5) left as fitting parameters except those with a star which are determined through fits with a fixed $\omega = 0.78$.

observable	L	ν	ω	χ^2/DOF
$\rho_s L$	$24 \leq L \leq 136$	0.708(5)	0.53(3)	1.6
$\rho_s L$	$32 \leq L \leq 136$	0.710(5)	0.57(5)	1.7
$\rho_s L$	$40 \leq L \leq 136$	0.711(6)	0.63(8)	1.7
$\rho_s L$	$24 \leq L \leq 96$	0.706(8)	0.48(5)	1.6
$\rho_s L$	$24 \leq L \leq 136$	0.711(7)*	N/A	2.0
$\rho_s L$	$32 \leq L \leq 136$	0.711(6)*	N/A	1.8
Q_2	$24 \leq L \leq 136$	0.710(5)	2.2(1)	0.9
Q_2	$32 \leq L \leq 136$	0.710(5)	2.42(25)	0.9
Q_2	$24 \leq L \leq 96$	0.712(7)	2.10(13)	1.0
Q_2	$24 \leq L \leq 136$	0.714(9)*	N/A	1.8
Q_2	$32 \leq L \leq 136$	0.712(7)*	N/A	1.2

TABLE III: The numerical values of ν and ω calculated from $\rho_s L$ and Q_2 for the herringbone-dimer model on the square lattice ($(J'/J)_c$ is fixed to 2.4980). All results are obtained by using a first order Taylor expansion in $tL^{1/\nu}$ of Eq. (5) with ω and b left as fitting parameters except those with a star which are determined through fits with a fixed $\omega = 0.78$.

tain is slightly below the expected $\omega \sim 0.78$ in the $O(3)$ universality class, hence is consistent with the scenario suggested in [22]. In particular, the correction to scaling due to the cubic term introduced in [22] reflects in the value of ω . This observation is in agreement with what we have obtained for the staggered-dimer model on the honeycomb lattice in previous section. However, these results for ω should only be considered as effective ones. Similarly, a fit using Q_2 with $24 \leq L \leq 136$ as well as a second order Taylor expansion in $tL^{1/\nu}$ of Eq. (5), with the confluent correction left as fitting parameters for the fit, leads to $(J'/J)_c = 2.49800(7)$ and $\nu = 0.714(4)$. Notice the determined $\nu = 0.714(4)$ is consistent with $\nu = 0.7112(5)$. Further, the confluent exponent ω from the fit is given by $\omega = 2.0(2)$. Finally, while using other range of L for Q_2 we can arrive at values of ν agreeing with $\nu = 0.7112(5)$, the ω calculated from these additional fits are poorly determined. Notice that a second order Taylor expansion in $tL^{1/\nu}$ of Eq. (5) with the subleading correction included for the fit contains seven fitting parameters, which is at the border of reasonable amount of the unknown coefficients for a fit. Still, one would like to understand whether a consistent ν with $\nu = 0.7112(5)$ can be obtained from the fits with fewer fitting parameters. Interestingly, using $(J'/J)_c = 2.4980$, the data points very close to the critical point, as well as a first order Taylor expansion in $tL^{1/\nu}$ of Eq. (5) with the confluent correction included explicitly (which has five unknown coefficients), the values of ν determined from these new fits for both $\rho_s L$ and Q_2 are compatible with $\nu = 0.7112(5)$ (table 3 and top panel of figure 4). Therefore we conclude that, our data points of $\rho_s L$ and Q_2 for the herringbone-dimer model on the square lattice indeed can be described nicely with the expected $\nu = 0.7112(5)$ in the $O(3)$ universality class. Notice that the values of ω calculated from the additional fits (first order Taylor expansion of Eq. (5)) related to $\rho_s L$ has an average of 0.55, hence again is in agreement with the scenario of a large correction to scaling for this phase transition induced by spatial anisotropy.

Interestingly, while the results we obtain so far are in consistence with the scenario that the cubic irrelevant term, which results in the observed enhanced correction to scaling, has impact on the confluent exponent ω , the numerical values of ν determined from the fits with a fixed $\omega = 0.78$ are also compatible with $\nu = 0.7112(5)$ for both $\rho_s L$ and Q (table 2 and table 3). For instance, a fit using a fixed $\omega = 0.78$ to the observable $\rho_s L$ with $32 \leq L \leq 96$ leads to $\nu = 0.707(3)$, which is in nice agreement with the expected result of $\nu = 0.7112(5)$. Further, we are also able to arrive at values of ν agreeing with $\nu = 0.7112(5)$ using the first order Taylor expansion in $tL^{1/\nu}$ of Eq. (5) with a fixed $\omega = 0.78$ for the fits (table 3). These additional fits contain only four unknown coefficients. Hence, both the strategies of fixing ω to be 0.78 or letting it be a fitting parameter lead to results of ν consistent with $\nu = 0.7112(5)$. Notice in our earlier calculations using a second order Taylor expansion of the

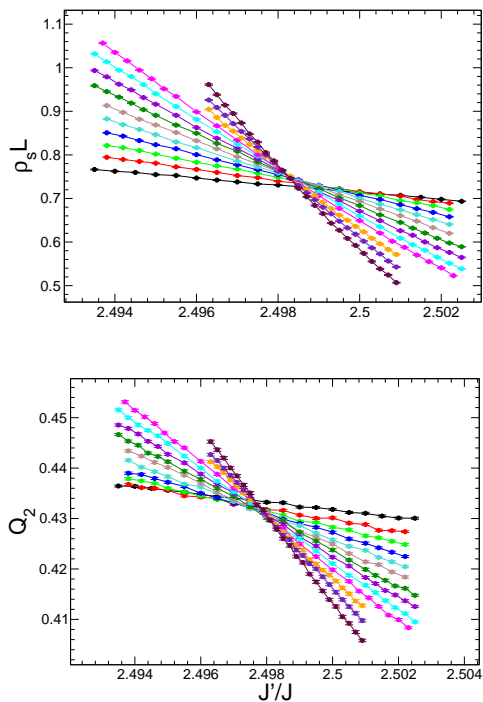


FIG. 3: Monte Carlo data of $\rho_s L$ and Q_2 with $24 \leq L \leq 136$ for the herringbone-dimer spin-1/2 Heisenberg model on the square lattice.

full ansatz Eq. (5), although the mean average of ω , determined from the fits with both the b and ω in Eq. (5) left as fitting parameters, is smaller than the expected 0.78 in most of the cases, the uncertainties for ω from these fits are large. Hence, for a spread range (a_1, a_2) of ω (i.e. $\omega \in (a_1, a_2)$), consistent ν with $\nu = 0.7112(5)$ is obtained from the fits using the chosen ω in (a_1, a_2). Therefore, it might be premature to conclude that the confluent exponent ω for this phase transition is smaller than 0.78 just from what we have obtained so far. In addition, since the values of ω obtained from the fits might be contaminated by higher order terms, a more sophisticated determination of ω should be performed. Indeed, as we will demonstrate later, by considering higher order corrections, the value of ω determined from the Q_2 data points of the herringbone-dimer model agrees reasonably well with $\omega \sim 0.78$.

C. Results for the ladder-dimer spin-1/2 Heisenberg model on the square lattice

The final dimer model considered in this study is the 2-d quantum Heisenberg model on the square lattice with a ladder spatial anisotropy, which has been studied extensively in the literature. Here for completeness, we have re-investigated the phase transition induced by dimerization of this model. Intuitively, due to their similarity, one might expect that the good scaling behavior of the

observable	L	ν	$(J'/J)_c$	χ^2/DOF
$\rho_{s1}2L$	$24 \leq L \leq 136$	0.707(2)	1.90955(9)	1.1
$\rho_{s1}2L$	$24 \leq L \leq 96$	0.705(3)	1.9096(2)	1.2
$\rho_{s1}2L$	$24 \leq L \leq 72$	0.696(5)	1.9095(6)	1.1
$\rho_{s1}2L$	$32 \leq L \leq 136$	0.708(2)	1.90956(12)	1.1
$\rho_{s1}2L$	$32 \leq L \leq 96$	0.706(3)	1.9097(2)	1.1
$\rho_{s1}2L$	$24 \leq L \leq 136$	0.706(2)*	1.90960(3)*	1.2
$\rho_{s1}2L$	$32 \leq L \leq 72$	0.698(5)*	1.90956(16)*	1.1
$\rho_{s1}2L$	$32 \leq L \leq 96$	0.707(3)*	1.90961(7)*	1.2
$\rho_{s1}2L$	$24 \leq L \leq 136$	0.704(3)	1.9095(1)	1.1
$\rho_{s1}2L$	$32 \leq L \leq 136$	0.705(3)	1.90956(13)	1.1

TABLE IV: The numerical values of ν and $(J'/J)_c$ calculated from $\rho_{s1}2L$ for the ladder-dimer model on the square lattice. While the results presented in the first eight rows are obtained by using a second order Taylor expansion in $tL^{1/\nu}$ of Eq. (5), those listed in the last two rows are determined with a third order Taylor expansion. Further, all results are calculated with the ω and b in Eq. (5) left as fitting parameters except those with a star which are determined through fits with a fixed $\omega = 0.78$.

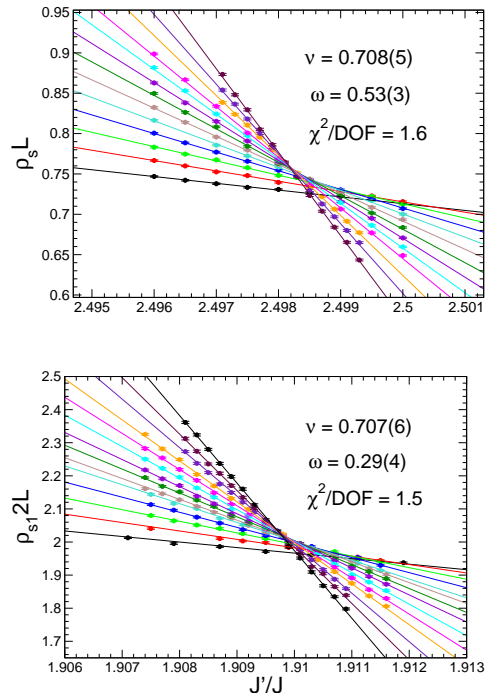


FIG. 4: Fits of $\rho_s L$ ($24 \leq L \leq 136$) of the herringbone-dimer model (top panel) and $\rho_{s1}2L$ ($24 \leq L \leq 136$) of the ladder-dimer model (bottom panel) to the first order Taylor expansion in $tL^{1/\nu}$ of the full ansatz Eq. (5). While the circles are the numerical Monte Carlo data from the simulations, the solid curves are obtained by using the results from the fits.

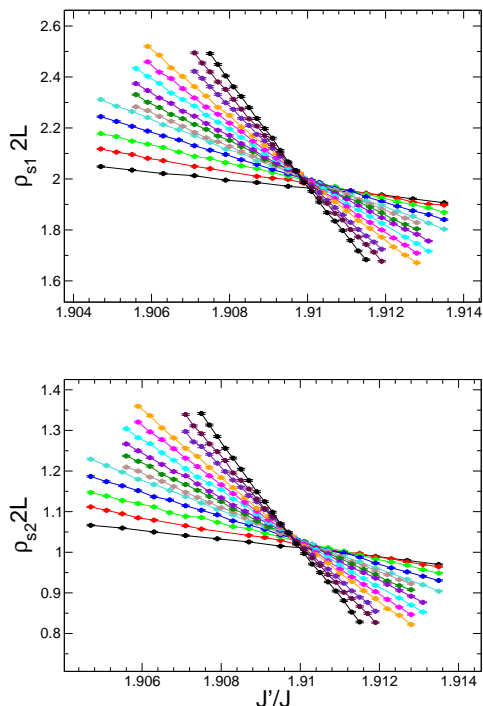


FIG. 5: Monte Carlo data of $\rho_{s1}2L$ and $\rho_{s2}2L$ with $24 \leq L \leq 136$ for the ladder-dimer spin-1/2 Heisenberg model on the square lattice.

observable	L	ν	ω	χ^2/DOF
$\rho_{s1}2L$	$24 \leq L \leq 136$	0.707(6)	0.29(4)	1.5
$\rho_{s1}2L$	$32 \leq L \leq 136$	0.709(6)	0.26(6)	1.5
$\rho_{s1}2L$	$24 \leq L \leq 96$	0.703(8)	0.28(6)	1.5

TABLE V: The numerical values of ν and ω calculated from $\rho_{s1}2L$ for the ladder-dimer model on the square lattice ($(J'/J)_c$ is fixed to 1.9095). All results are obtained by using a first order Taylor expansion in $tL^{1/\nu}$ of the full ansatz Eq. (5).

observable $\rho_{s2}2L$, found for the staggered-dimer model on both the square and honeycomb lattices, will emerge again for the ladder-dimer model. Interestingly, the effects of the correction to scaling for $\rho_{s1}2L$ and $\rho_{s2}2L$ of this model are about the same qualitatively (figure 4). This indicates the fundamental difference regarding the correction to scaling between the staggered- and ladder-dimer models as suggested in [22]. Similar to the analysis performed for obtaining ν and $(J'/J)_c$ for the herringbone-dimer model, a second order Taylor expansion in $tL^{1/\nu}$ of Eq. (5), with the subleading correction included explicitly, is employed to fit the Monte Carlo data of $\rho_{s1}2L$ with variant range of L . The obtained $(J'/J)_c$ and ν are in table 4. Interestingly, table 4 implies that a result for ν compatible with $\nu = 0.7112(5)$ can be ob-

tained as well if the smallest and largest box sizes used in the fits are larger than 24 and 96, respectively. Further, although with considerable large uncertainties, most the values of ω determined from these fits are smaller than 0.78 and are compatible in magnitude with those determined from the herringbone-dimer model. In addition, using $(J'/J)_c = 1.9095$, the data points very close to the critical point, as well as a first order Taylor expansion in $tL^{1/\nu}$ of the full ansatz Eq. (5), the values of ν determined from these new fits for $\rho_{s1}2L$ are compatible with $\nu = 0.7112(5)$ (table 5 and bottom panel of figure 4). Therefore we conclude that, our data points of $\rho_{s1}2L$ for the ladder-dimer model on the square lattice indeed can be described nicely with the expected $\nu = 0.7112(5)$ in the $O(3)$ universality class. Finally, similar to the results for the herringbone-dimer model, with a fixed $\omega = 0.78$, the values of ν calculated from our finite-size scaling analysis are compatible with $\nu = 0.7112(5)$ as well (table 4).

IV. DETERMINATION OF THE EXPONENT β/ν

After having calculated the critical exponent ν from the relevant observables for the models described by figure 1, we turn to the determination of the exponent β/ν . To calculate β/ν , the scaling behavior of the observables $\langle |m_s^z| \rangle$ and $\langle (m_s^z)^2 \rangle$ are studied. Specifically, at critical points and for large L , the observable $\langle |m_s^z|^k \rangle$ should scale as

$$\langle |m_s^z|^k \rangle = (a_k + b_k L^{-\omega}) L^{-k\beta/\nu}, \quad (6)$$

where a_k, b_k are some constants for $k = 1$ and each even positive integer k . Since precise knowledge of the critical points is essential in determining the exponent β/ν , we use the values of $(J'/J)_c$ obtained in previous sections when calculating the critical exponent ν . Interestingly, as shown in tables 1, 2, and 4, small statistical deviation between some of the determined critical points of the same model is found. We attribute such small discrepancy to the presence of higher order subleading corrections which are not taken into account in our analysis, as well as the fact that the bootstrap resampling method used in calculating $(J'/J)_c$ and ν might occasionally leads to underestimated errors. While small deviation is observed, the accuracy of $(J'/J)_c$ presented in tables 1, 2, and 4, is sufficient for determining β/ν by investigating the scaling behavior of $\langle |m_s^z| \rangle$ and $\langle (m_s^z)^2 \rangle$, at the corresponding critical points. Hence, the values of $(J'/J)_c$ for the herringbone- and ladder-dimer models on the square lattice, as well as the staggered-dimer model on the honeycomb lattice are taken to be 2.4980, 1.9095, and 1.7355, respectively. Further, we have carried out additional simulations at these critical points so that the largest lattice size we reach for both the herringbone- and staggered-dimer models is $L = 184$. First of all, let us focus on the results of β/ν obtained from $\langle |m_s^z| \rangle$. Interestingly, with the expected leading scaling behavior,

only from the ladder-dimer model we are able to reach a value of β/ν which is in agreement with the established result $\beta/\nu = 0.519(1)$ in the literature. For example, while a fit using the leading scaling expectation and the observable $\langle |m_s^z| \rangle$ with $L \geq 72$ of the ladder-dimer model results in $\beta/\nu = 0.517(2)$ (top panel of figure 6), the corresponding numerical value of β/ν determined from the same observable, with a similar range of L , is given by $\beta/\nu = 0.527(3)$ ($\beta/\nu = 0.531(3)$) for the herringbone-dimer model (staggered-dimer model on the honeycomb lattice). Further, using $L \geq 128$ ($L \geq 120$), the value of β/ν obtained from a fit without the confluent correction for the herringbone-dimer model (staggered-dimer model on the honeycomb lattice) is given by $\beta/\nu = 0.522(5)$ ($\beta/\nu = 0.526(3)$). From this outcome and in conjunction with the results reached from previous sections, one concludes that the correction to scaling for the staggered- and herringbone-dimer models are indeed enhanced as proposed in [22]. In particular, the effect of the correction to scaling due to the cubic term is the reduction of the magnitude of the confluent exponent ω . Surprisingly, for both the herringbone-dimer model on the square lattice and the staggered-dimer model on the honeycomb lattice, using the data of $\langle |m_s^z| \rangle$ with $16 \leq L \leq 184$, a fit including the subleading correction and a fixed $\omega = 0.78$ leads to values of β/ν compatible with $\beta/\nu = 0.519(1)$ (middle and bottom panels of figure 6). Further, if ω is left as a fitting parameter, although consistent β/ν with $\beta/\nu = 0.519(1)$ are obtained from the fits associated with the herringbone-dimer model, the uncertainties for β/ν and ω are increased significantly. For example, the β/ν and ω determined from a fit using $\langle |m_s^z| \rangle$ with $16 \leq L \leq 184$ of the herringbone-dimer model are given by $\beta/\nu = 0.521(9)$ and $0.86(50)$, respectively. Finally, a fit to the observable $\langle |m_s^z| \rangle$ of the ladder-dimer model with a fixed $\omega = 0.78$ leads to $\beta/\nu = 0.516(3)$, which is consistent with $\beta/\nu = 0.519(1)$ as well. Interestingly, a value of β/ν slightly below $\beta/\nu = 0.519(1)$ is reached when the leading scaling prediction is employed to fit all available data of $\langle |m_s^z| \rangle$ of the ladder-dimer model. This in turn implies that the coefficient b_1 in Eq. (6) for the ladder-dimer model is small in magnitude. Indeed, the magnitude of b_1 obtained from applying the full ansatz Eq. (6) with a fixed $\omega = 0.78$ to $\langle |m_s^z| \rangle$ of the ladder-dimer model is of order 10^{-2} (The uncertainty for b_1 is comparable to b_1 in magnitude as well). Finally, we have also carried out an additional analysis with different fixed values of ω in the fits. The obtained β/ν for these additional fits are shown in table 7. From table 7 one concludes that the values of ω that would lead to consistent β/ν with $\beta/\nu = 0.519(1)$ for both the herringbone- and staggered-dimer models ranges from 0.7 to 0.9, which matches reasonable well with the expected value 0.78. All the results we have reached so far imply that, our data points of $\langle |m_s^z| \rangle$ for all the three dimerized models depicted in figure 1 are compatible with the established value of $\omega \sim 0.78$ in the $O(3)$ universality class.

After having demonstrated that our Monte Carlo data

model	L	β/ν	χ^2/DOF
ladder	$72 \leq L \leq 136$	$0.517(2)^*$	0.75
ladder	$16 \leq L \leq 136$	$0.516(3)$	1.1
herringbone	$72 \leq L \leq 136$	$0.527(3)^*$	1.5
herringbone	$128 \leq L \leq 184$	$0.522(5)^*$	0.7
herringbone	$16 \leq L \leq 184$	$0.520(2)$	1.0
staggered	$72 \leq L \leq 136$	$0.531(3)^*$	1.2
staggered	$120 \leq L \leq 184$	$0.526(3)^*$	0.55
staggered	$16 \leq L \leq 184$	$0.518(2)$	1.35
ladder	$88 \leq L \leq 136$	$0.515(2)^*$	0.45
ladder	$16 \leq L \leq 136$	$0.515(2)$	1.3
herringbone	$128 \leq L \leq 184$	$0.525(4)^*$	1.25
herringbone	$16 \leq L \leq 184$	$0.5202(15)$	1.0
staggered	$128 \leq L \leq 184$	$0.527(4)^*$	1.1
staggered	$16 \leq L \leq 184$	$0.518(2)$	1.4

TABLE VI: The numerical values of β/ν calculated from $\langle |m_s^z| \rangle$ (the first 8 rows) and $\langle (m_s^z)^2 \rangle$ (the last 6 rows) for the dimerized models considered in this study. All results are obtained with a fixed $\omega = 0.78$ except those with a star which are determined by using the expected leading scaling prediction.

of $\langle |m_s^z| \rangle$, for all the three dimerized models investigated here, are compatible with the established results of $\beta/\nu = 0.519(1)$ and $\omega = 0.78$ in the $O(3)$ universality class, a similar scenario is reached when considering the observable $\langle (m_s^z)^2 \rangle$. For example, using the leading scaling prediction, only from the ladder-dimer model we can reach a value for β/ν compatible with $\beta/\nu = 0.519(1)$ (top panel of figure 7). Further, with a fixed $\omega = 0.78$, the fits for the herringbone-dimer model on the square lattice and the staggered-dimer model on the honeycomb lattice result in $\beta/\nu = 0.5202(15)$ and $\beta/\nu = 0.518(2)$, respectively (middle and bottom panels of figure 7). The results of $\beta/\nu = 0.5202(15)$ and $\beta/\nu = 0.518(2)$ we just obtain are in quantitative agreement with the expected $\beta/\nu = 0.519(1)$. Further, an analysis for $\langle (m_s^z)^2 \rangle$, with variant fixed values of ω in the fits, leads to a similar conclusion like that of $\langle |m_s^z| \rangle$. Specifically, from $\langle (m_s^z)^2 \rangle$, the values of ω that would lead to consistent β/ν with $\beta/\nu = 0.519(1)$ for both the herringbone- and staggered-dimer models ranges from 0.7 to 0.9 as well (table 8). Tables 6, 7, and 8 summarizes our calculations on determining β/ν for the phase transitions induced by dimerization for all the three models shown in figure 1.

V. DETERMINATION OF THE EXPONENT ω

In previous sections, the numerical values of ω are poor determined. Here we attempt to have better estimates for the confluent exponent ω of both the herringbone- and staggered-dimer models. As a first step toward ful-

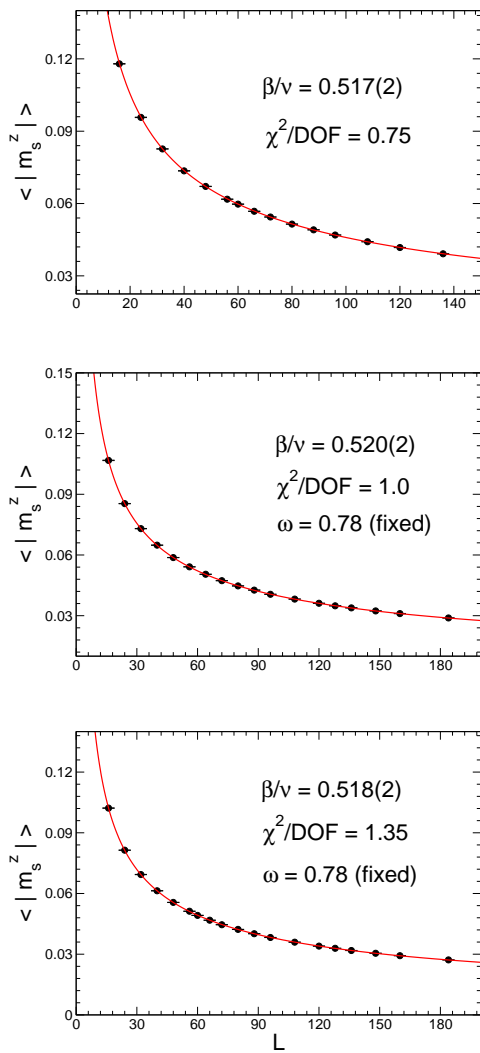


FIG. 6: Determination of β/ν for the ladder- and herringbone-dimer models (top and middle panels) on the square lattice as well as for the staggered-dimer model on the honeycomb lattice (bottom panel). While $\beta/\nu = 0.517(2)$ for the ladder-dimer model is obtained by fitting the 7 largest L data points of $\langle |m_s^z| \rangle$ to their expected leading scaling behavior, fits with a fixed $\omega = 0.78$ to $\langle |m_s^z| \rangle$ of the herringbone-dimer model on the square lattice and the staggered-dimer model on the honeycomb lattice result in $\beta/\nu = 0.520(2)$ and $\beta/\nu = 0.518(2)$, respectively.

for this purpose, let us reanalyze our $\langle |m_s^z| \rangle$ data of the herringbone- and staggered-dimer models from another point of view. Notice the values of ω and β/ν are poorly determined when both of them are included as fitting parameters for the fits. Interestingly, for both the herringbone- and staggered-dimer models, if we fix β/ν to the known result $\beta/\nu = 0.519$ in the literature, then the ω we obtain from these new fits are much better determined and are in nice agreement with $\omega \sim 0.78$. For example, for the herringbone-dimer (staggered-dimer) model, using a fixed $\beta/\nu = 0.519$, we arrive at $\omega = 0.74(8)$

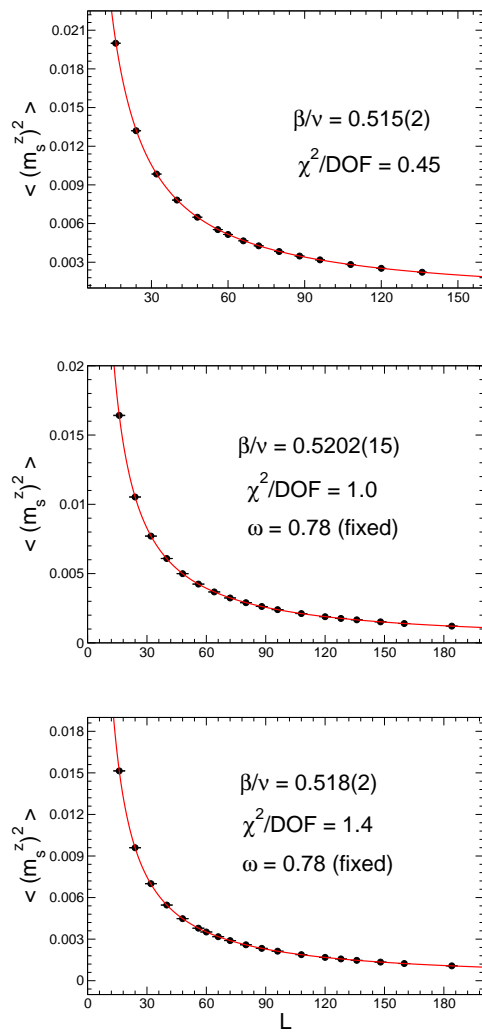


FIG. 7: Determination of β/ν for the ladder- and herringbone-dimer models (top and middle panels) on the square lattice as well as for the staggered-dimer model on the honeycomb lattice (bottom panel). While $\beta/\nu = 0.515(2)$ for the ladder-dimer model is obtained by fitting the 5 largest L data points of $\langle (m_s^z)^2 \rangle$ to their expected leading scaling behavior, fits with a fixed $\omega = 0.78$ to $\langle (m_s^z)^2 \rangle$ of the herringbone-dimer model on the square lattice and the staggered-dimer model on the honeycomb lattice result in $\beta/\nu = 0.5202(15)$ and $\beta/\nu = 0.518(2)$, respectively.

($\omega = 0.80(5)$). Summarizing all the analysis done so far related to the observables $\langle |m_s^z| \rangle$ and $\langle (m_s^z)^2 \rangle$, we conclude that our these data points are fully compatible with the known results of $\beta/\nu = 0.519(1)$ and $\omega \sim 0.78$ in the $O(3)$ universality class. Next, we will focus on the finite-size scaling analysis of Q_2 and $\rho_s L$ at the corresponding critical points. First of all, let us discuss the results for the herringbone-dimer model. Notice, at critical points, the finite-size scaling ansatz for Q_2 (and $\rho_s L$ as well) is given as

$$Q_2 = a + bL^{-\omega} + cL^{-2\omega} + \dots, \quad (7)$$

model	$\omega(\text{fixed})$	β/ν	χ^2/DOF
herringbone	1.0	0.523(2)	1.0
herringbone	0.9	0.522(2)	1.0
herringbone	0.7	0.5181(23)	1.06
herringbone	0.65	0.5168(25)	1.05
herringbone	0.6	0.5152(27)	1.04
herringbone	0.45	0.5078(36)	1.05
staggered	1.0	0.523(2)	1.55
staggered	0.9	0.521(2)	1.46
staggered	0.7	0.5150(25)	1.3
staggered	0.65	0.5127(25)	1.23
staggered	0.6	0.5101(25)	1.2
staggered	0.45	0.4974(35)	1.15

TABLE VII: The numerical values of β/ν calculated from $\langle |m_s^z| \rangle$ ($16 \leq L \leq 184$) with variant fixed ω for the fits.

model	$\omega(\text{fixed})$	β/ν	χ^2/DOF
herringbone	1.0	0.5232(12)	1.03
herringbone	0.9	0.5221(13)	1.0
herringbone	0.7	0.5185(15)	1.0
herringbone	0.65	0.5172(16)	1.0
herringbone	0.6	0.5156(18)	1.05
herringbone	0.45	0.5082(25)	1.1
staggered	1.0	0.5235(15)	1.7
staggered	0.9	0.5213(15)	1.55
staggered	0.7	0.515(2)	1.4
staggered	0.65	0.512(2)	1.35
staggered	0.6	0.509(2)	1.35
staggered	0.45	0.4920(36)	1.5

TABLE VIII: The numerical values of β/ν calculated from $\langle (m_s^z)^2 \rangle$ ($16 \leq L \leq 184$) with variant fixed ω for the fits.

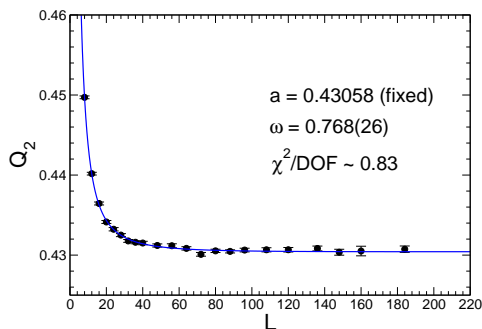


FIG. 8: Fit of Q_2 data ($8 \leq L \leq 184$) of the herringbone-dimer model to Eq. (7).

where a, b, c are some constants and “...” in Eq. (7) stands for higher order corrections. In addition to the corrections associated with the confluent exponent ω , there are other subleading corrections with exponents $\omega' > \omega$. Notice that since the established values of ω' are larger or equal to 2ω , it is reasonable to employ the scaling ansatz Eq. (7) for data analysis. From our data of Q_2 for the herringbone-dimer model, we observe two interesting results as follows. First, Q_2 converges rapidly to a constant. Indeed, for $64 \leq L \leq 184$, an average of the corresponding values of Q_2 leads to $Q_2 = 0.43058(22)$, where the quoted error is obtained by the variance of these Q_2 . Second, we find that when the ansatz with only the leading correction is employed for the fits, then the values of ω calculated are much larger than the expected $\omega \sim 0.78$ in the $O(3)$ universality class. For example, a fit using Eq. (7) up to the term $bL^{-\omega}$ and the data points of $4 \leq L \leq 136$ ($8 \leq L \leq 120$) leads to $\omega \sim 1.74$ ($\omega \sim 1.69$), with a $\chi^2/\text{DOF} = 1.29$ ($\chi^2/\text{DOF} = 1.2$). These results indicate that the influence of higher order terms already sets in. Hence, instead of using the ansatz with only the leading correction term, the term of $cL^{-2\omega}$ in Eq. (7) should be additionally included in the fits. Remarkably, with a fixed $a = 0.43058$ in Eq. (7), the ω determined from the fits employing the ansatz $0.43058 + bL^{-\omega} + cL^{-2\omega}$ are compatible with the expected $\omega \sim 0.78$. For instance, from a fit using the Q_2 data with $8 \leq L \leq 184$, we arrive at $\omega = 0.768(26)$ which agrees nicely with $\omega = 0.78(1)$. The top 6 rows of table 9 summarize the results of these fits employing the Q_2 data with different range of L , and fig. 8 demonstrates one outcome of these fits. Notice in table 9, if the coefficient a in Eq. (7) is left as a fitting parameter, then from the Q_2 data, the values of ω are less accurately determined and are with large errors, but still they are in reasonable agreement with $\omega \sim 0.78$. Similarly, by considering the observable $\rho_s L$ at the critical point, fits of applying Eq. (7) to $\rho_s L$ data points lead to consistent ω with $\omega = 0.78(1)$, see the bottom 4 rows of table 9 as well as fig. 9. Interestingly, when the a in Eq. (7) is left as an unknown parameter for the fits, then the values of ω , obtained from the observable $\rho_s L$, are in better agreement with $\omega \sim 0.78$ than those determined from Q_2 . From our finite-size scaling analysis on Q_2 and $\rho_s L$ at the critical point, we conclude that in previous section, the obtained values of ω are deviated from $\omega \sim 0.78$ significantly because they are contaminated by higher order corrections. This is confirmed by the fact that, our reinvestigation of $\rho_s L$ (Q_2) data close to the critical point, using first order Taylor expansion of Eq. (5) as well as including the correction $b_1 L^{-2\omega}$ in the fitting ansatz, leads to $\nu = 0.709(3)$, $\omega \sim 0.8$ ($\nu = 0.710(5)$, $\omega \sim 0.82$) with a $\chi^2/\text{DOF} = 1.57$ ($\chi^2/\text{DOF} = 0.82$). In conclusion, for the herringbone-dimer model, the values of ω we obtain from the finite-size scaling analysis are in quantitative consistence with the known $O(3)$ result $\omega = 0.78(1)$.

After having shown that the numerical values of ω calculated from the Q_2 and $\rho_s L$ data points of the

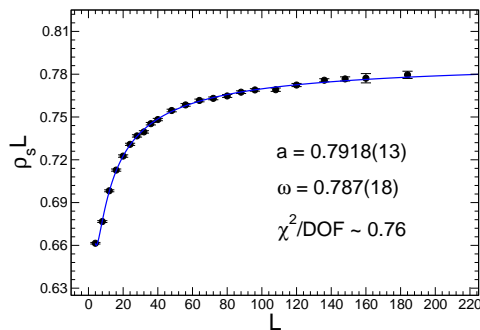


FIG. 9: Fit of $\rho_s L$ data ($4 \leq L \leq 184$) of the herringbone-dimer model to Eq. (7).

herringbone-dimer model agree nicely with the expected $\omega \sim 0.78$ in the $O(3)$ universality class, we turn to determining the exponent ω of the staggered-dimer model on the honeycomb lattice. The observables Q_2 and $\rho_s L$ are used as well. Interestingly, while for the herringbone-dimer model, the observable Q_2 converges rapidly to a constant, this is not the case for the staggered-dimer model. As a result, a in Eq. (7) must be left as one fitting parameter. Table 10 summarizes the results of these fits associated with the staggered-dimer model, and fig. 10 shows one outcome of these fits. Notice the obtained results of ω in table 10 are slightly below $\omega \sim 0.78$ (This also occurs for some results associated with the herringbone-dimer model). It is anticipated that the deviation between the values of ω in table 10 and $\omega \sim 0.78$ will not lead to the large correction to scaling known in the literature for this model. Hence we attribute the observed small differences between the results of ω shown in table 10 and $\omega = 0.78(1)$ to higher order corrections not taken into account in our analysis. Surprisingly, when we perform a similar analysis for the observable $\rho_{s1}L$, the values of ω we obtain are significantly lower than $\omega \sim 0.78$. There are several possible explanations for this observation, for instance, $\rho_{s1}L$ is sensible to the critical point. A thorough determination of ω for the staggered model, including considering the uncertainties of the critical point, studying other relevant observables, as well as employing the idea of fixing the aspect ratio of winding numbers squared (Notice the spatial winding numbers squared in 1- and 2-directions take the same values automatically for the herringbone-dimer model), will be left for future work.

VI. DISCUSSION AND CONCLUSION

In this study, we investigate the phase transitions induced by dimerization for the herringbone- and ladder-dimer spin-1/2 Heisenberg model on the square lattice, as well as the staggered-dimer model on the honeycomb lattice. In particular, we determine the values of the exponents ν and β/ν with high accuracy by employing

Observable	L	a	ω	χ^2/DOF
Q_2	$8 \leq L \leq 184$	0.43058(fixed)	0.768(26)	0.83
Q_2	$8 \leq L \leq 120$	0.43058(fixed)	0.760(26)	0.89
Q_2	$8 \leq L \leq 96$	0.43058(fixed)	0.751(26)	0.92
Q_2	$8 \leq L \leq 184$	0.4312(6)	0.693(56)	0.78
Q_2	$8 \leq L \leq 120$	0.4310(7)	0.708(67)	0.92
Q_2	$8 \leq L \leq 96$	0.4307(7)	0.738(82)	1.0
$\rho_s L$	$4 \leq L \leq 184$	0.7918(13)	0.787(18)	0.76
$\rho_s L$	$4 \leq L \leq 136$	0.7912(14)	0.794(19)	0.81
$\rho_s L$	$8 \leq L \leq 136$	0.794(3)	0.732(57)	0.76
$\rho_s L$	$8 \leq L \leq 88$	0.794(5)	0.737(77)	0.66

TABLE IX: The numerical values of ω , calculated from the observables Q_2 and $\rho_s L$ at the critical point, for the herringbone-dimer model on the square lattice. The ansatz used for the fits is $a + bL^{-\omega} + cL^{-2\omega}$.

Observable	L	a	ω	χ^2/DOF
Q_2	$4 \leq L \leq 136$	0.4317(3)	0.719(12)	0.98
Q_2	$4 \leq L \leq 88$	0.4315(4)	0.725(13)	1.04
Q_2	$4 \leq L \leq 184$	0.4319(3)	0.714(10)	0.98
Q_2	$6 \leq L \leq 136$	0.4321(5)	0.698(21)	0.96
Q_2	$6 \leq L \leq 88$	0.4319(6)	0.704(25)	1.05
Q_2	$6 \leq L \leq 184$	0.4324(5)	0.688(18)	0.92

TABLE X: The numerical values of ω , calculated from the observable Q_2 at the critical point, for the staggered-dimer model on the honeycomb lattice. The ansatz used for the fits is $a + bL^{-\omega} + cL^{-2\omega}$.

the finite-size scaling analysis to the relevant observables. Similar to the scenario found for the staggered-dimer model on the square lattice, while the observable $\rho_{s1}2L$ of the staggered-dimer model on the honeycomb lattice receives a sizable correction to its scaling, the observable $\rho_{s2}2L$ shows a good scaling behavior. As a result, us-

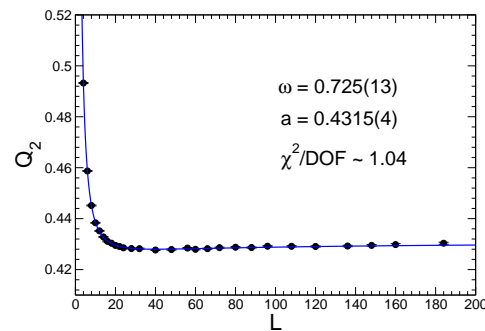


FIG. 10: Fit of Q_2 data of the staggered-dimer model to Eq. (7). The results is obtained by using the data with $4 \leq L \leq 88$.

ing the data points of $\rho_s 2L$ with moderate lattice sizes as well as the corresponding leading finite-size scaling ansatz (letting $b = 0$ in Eq. (5)), we are able to obtain a value for ν consistent with the expected $\nu = 0.7112(5)$ in the $O(3)$ universality class. To understand this observation for the staggered-dimer model on both the square and honeycomb lattices from field theory aspect, is an interesting and important topic to explore. In particular, whether the cubic term introduced in [22] is responsible for this unexpected result should be investigated. Further, while it is argued in [22] that the herringbone-dimer model belongs to the category of models receiving a large correction, and our investigation supports this scenario, we find that the cubic term most likely has little influence on the confluent exponent ω . In particular, our Monte Carlo data of $\rho_s L$ as well as Q_2 are compatible with the established result of $\omega \sim 0.78$ in the $O(3)$ universality class, namely with a fixed $\omega = 0.78$, we are able to arrive at consistent ν with $\nu = 0.7112(5)$ from both $\rho_s L$ and Q_2 of the herringbone-dimer model. In order to clarify whether the cubic term introduced in [22] has no impact on the numerical value of ω , it will be desirable to carry out a more detailed investigation to determine ω with high precision. In particular, the consistence of the ν , obtained from the fits using a fixed $\omega = 0.78$, with $\nu = 0.7112(5)$ as shown in tables 2, 3, 4 and 5, is unlikely a coincidence considering the fact that the conclusion is valid for both the observables spin stiffness and second Binder ratio of both the herringbone- and ladder-dimer models. In addition, the finite-size scaling analysis performed for the determination of β/ν suggests that, our data points for all the 2-d dimerized models with spatial anisotropy considered here are compatible with the established results of $\beta/\nu = 0.519(1)$ and $\omega \sim 0.78$ in the $O(3)$ universality class as well. Finally, the consistence of the β/ν , determined from the fits using a fixed $\omega \in \{0.7, 0.9\}$, with $\beta/\nu = 0.519(1)$ implies that the observed enhanced correction to both the staggered- and herringbone-dimer models is because of the nonuniversal coefficients b_k in Eq. (6). Indeed, in tables 6, 7, and 8, the values of b_1 and b_2 determined from the fits associated with the herringbone- and staggered-dimer models are at least several times larger in magnitude than those of the ladder-dimer model (This conclusion remains valid when considering the data sets generated using lower temperatures). It is interesting to notice that the slopes of χ_u/T as functions of T/J when approaching the low-temperature regime (χ_u is the uniform susceptibility), as shown in the figure 6 of [22], imply that the correction for the staggered- and herringbone-dimer models are large when compared to those of the ladder- and bilayer-

dimer models. This can be considered as a analogy to our results for $\langle |m_s^z| \rangle$ and $\langle (m_s^z)^2 \rangle$, and might be used as another evidence for the scenario that the influence on the scaling due to the cubic term is the amplification of the nonuniversal prefactors appeared in the scaling forms. Whether there is a subtlety behind the results for $\langle |m_s^z| \rangle$ and $\langle (m_s^z)^2 \rangle$ shown here and the uniform susceptibilities presented in [22], or it is just a coincidence should be investigated analytically. Indeed, we have shown that the values of ω for the herringbone- and staggered-dimer model agree reasonably well with $\omega \sim 0.78$, by studying the scaling behavior of Q_2 and $\rho_s L$ at the corresponding critical points. The rapid saturation of the observable Q_2 to a constant is crucial in leading to a precise determination of ω for the herringbone-dimer model. While the accuracy for ω presented here has not reached the same level of $\omega = 0.78(1)$, we have obtained sufficiently good precision for ω to draw the above conclusions. Our study of calculating the values of ω through Q_2 and $\rho_s L$, at least for the herringbone-dimer model, at the critical points reinforces our proposed scenario that the enhanced correction to scaling manifests itself as amplification of the nonuniversal prefactors appeared in the scaling forms. While we demonstrate strong evidence that for the herringbone- and staggered-dimer models, the exponents ν , β/ν , as well as ω agree quantitatively with the established results in the $O(3)$ universality class, still, our estimates for the numerical value of ω are of a few percent uncertainties. Further, the exponent ω is associated with the correction to scaling, and to accurately determine its value is of highly nontrivial. Hence one cannot rule out the scenario that indeed the values of ω is reduced (slightly) due to the cubic term. Hence it is desirable to obtain high statistics data points in order to reach a even higher precision determination of ω for the models investigated here [39]. In light of this, as well as the fact that the values of ω calculated from $\rho_{s1} L$ of the staggered-dimer model are lower than (and statistically different from) the expected $\omega \sim 0.78$, a more detailed numerical study (to determine the confluent exponent ω) and a better theoretical understanding, for the critical theories of the phase transitions investigated here will be very useful.

VII. ACKNOWLEDGMENTS

We thank S. Wessel for useful correspondence. Partial support from NSC (Grant No. NSC 99-2112-M003-015-MY3) and NCTS (North) of R.O.C. is acknowledged.

-
- [1] M. Matsumoto, C. Yasuda, S. Todo, and H. Takayama, Phys. Rev. B **65**, 014407 (2001)
 [2] M. Troyer, Prog. Theor. Phys. Supp. **145**, 326 (2002).
 [3] L. Wang, K. S. D. Beach, and A. W. Sandvik, Phys. Rev.

- B **73**, 014431 (2006).
 [4] C. Yasuda *et al.*, Phys. Rev. Lett. **94**, 217201 (2005).
 [5] M. B. Hastings and C. Murdry, Phys. Rev. Lett. **96**, 027215 (2006).

- [6] A. Praz, C. Murdy, and M. B. Hastings, Phys. Rev. B **74**, 184407 (2006).
- [7] D. X. Yao and A. W. Sandvik, Phys. Rev. B **75**, 052411 (2007).
- [8] K. H. Höglund, A.W. Sandvik, and S. Sachdev, Phys. Rev. Lett. **98**, 087203 (2007).
- [9] K. H. Höglund and A.W. Sandvik, Phys. Rev. Lett. **99**, 027205 (2007)
- [10] T. Pardini, R. R. P. Singh, A. Katanin and O. P. Sushkov, Phys. Rev. B **78**, 024439 (2008).
- [11] F.-J. Jiang, F. Kämpfer, and M. Nyfeler, Phys. Rev. B **80**, 033104 (2009).
- [12] S. Jin and A. W Sandvik, arXiv:1110.5347.
- [13] J. Oitmaa, Y. Kulik, and O. P. Sushkov, arXiv:1110.6478.
- [14] S. Wenzel, L. Bogacz, and W. Janke, Phys. Rev. Lett. **101**, 127202 (2008).
- [15] S. Chakravarty, B. I. Halperin, and D. R. Nelson, Phys. Rev. Lett. **60**, 1057 (1988).
- [16] F. D. M. Haldane, Phys. Rev. Lett. **61**, 1029 (1988).
- [17] A. V. Chubukov, S. Sachdev, and J. Ye, Phys. Rev. B **49**, 11919 (1994).
- [18] S. Sachdev, *Quantum Phase Transitions* (Cambridge University Press, Cambridge, 1999).
- [19] M. Vojta, Rep. Prog. Phys. **66**, 2069 (2003).
- [20] M. Campostrini, M. Hasenbusch, A. Pelissetto, P. Rossi, and E. Vicari, Phys. Rev. B **65**, 144520 (2002).
- [21] F.-J. Jiang, Rev. B **85** 014414 (2012).
- [22] L. Fritz et al., Phys. Rev. B **83**, 174416 (2011)
- [23] M. Matsumoto, C. Yasuda, S. Todo, and H. Takayama, Phys. Rev. B **65**, 014407 (2001)
- [24] A. F. Albuquerque, M. Troyer, and J. Oitmaa, Phys. Rev. B **78**, 132402 (2008).
- [25] S. Wenzel and W. Janke, Phys. Rev. B **79**, 014410 (2009).
- [26] F.-J. Jiang and U. Gerber, J. Stat. Mech. P09016 (2009).
- [27] A work of determining β/ν is available in “S. Wenzel, PhD thesis, Universität Leipzig (2009)”.
- [28] A work of studying the critical theory for the herringbone-dimer model is available in “S. Wenzel, PhD thesis, Universität Leipzig (2009)”.
- [29] H. G. Evertz, G. Lana, and M. Marcu, Phys. Rev. Lett. **70**, 875 (1993).
- [30] H. G. Evertz, Adv. Phys. **52**, 1 (2003).
- [31] U.-J. Wiese and H.-P. Ying, Z. Phys. B **93**, 147 (1994).
- [32] B. B. Beard and U.-J. Wiese, Phys. Rev. Lett. **77** (1996) 5130.
- [33] A. F. Albuquerque et. al, Journal of Magnetism and Magnetic Material 310, 1187 (2007).
- [34] M. E. Fisher and M. N. Barber, Phys. Rev. Lett. **28**, 1516 (1972).
- [35] E. Brézin, J. Phys. (Paris) **43**, 15 (1982).
- [36] M. N. Barber, in *Phase Transitions and Critical Phenomena*, ed. C. Domb (Academic, New York, 1983), Vol. 8.
- [37] E. Brézin and J. Zinn-Justin, Nucl. Phys. B **257**, 867 (1985).
- [38] M. P. A. Fisher, P. B. Weichman, G. Grinstein, and D. S. Fisher, Phys. Rev. B **40**, 546 (1989).
- [39] M. Hasenbusch, J. Phys. A 32, 4851-4865, 1999.